Metal–Organic Frameworks with Boronic Acid Suspended and Their Implication for *cis*-Diol Moieties Binding

Xiangyang Zhu, Jinlou Gu, Junying Zhu, Yongsheng Li, Liming Zhao, and Jianlin Shi*

Introduction of accessible boronic acid functionality into metal–organic frameworks (MOFs) might to endow them with desired properties for potential applications in recognition and isolation of *cis*-diol containing biomolecules (CDBs). However, no investigation is found to address this topic until now. Herein, Cr-based MOFs of MIL-100 (MIL stands for Materials from Institut Lavoisier) integrated with different pendent boronic acid group (MIL-100-B) are reported. This new functional material is successfully prepared using a simple metal–ligand–fragment coassembly (MLFC) strategy with isostructure to the parent MIL-100 as verified by X-ray diffraction characterization. The integration and content tunability of the boronic acid group in the framework are confirmed by X-ray photoelectron spectroscopy and ^{11}B NMR. Transmission electron microscopy reveals that MIL-100-B can evolve into well-defined morphology and nanoscale size at optimized boronic acid incorporating level. The obtained MOFs exhibit comparable surface areas and pore volumes with parent MIL-100 and present exceptional chemical stability in a wide pH range. The inherent boronic acid components in MIL-100-B can effectively serve as the recognition units for the *cis*-diol moieties and consequently enhance the capture capabilities for CDBs. The exceptional chemical stability, high porosity, and good reusability as well as the intrinsic *cis*-diol moieties recognition function prefigure great potential of the current MIL-100-B in CDBs purification, sensing, and separation applications.

1. Introduction

Cis-diol containing biomolecules (CDBs), such as saccharides,[1,2] glycoproteins,[3,4] catechols,[5] and nucleosides[6] play significant roles in many biological processes. It is consequently essential to develop reliable approaches for their efficient recognition and separation. To date, several strategies have been proposed, among which boronate-based affinity isolation has drawn increasing research interest.[7–10] The excellent affinity of boronic acids towards CDBs relies on the fact that they could form stable cyclic esters with *cis*-diol moieties in mild basic or neutral aqueous solution, while the cyclic esters dissociate once switching the medium to acidic pH.[11,12] Considerable efforts have been devoted to constructing boronate-functionalized materials,[13–16] especially porous functional materials,[17–20] for the specific recognition and subsequent isolation of CDBs from biological samples. However, in most cases, multistep synthesis procedures with harsh reaction conditions were generally needed to modify boronic acid on the surface of applied materials. Besides, they sometime suffered from the low conjugation efficiency of boronic acid and inhomogeneous surface coverage that might be also the limitations for their practical applications. Therefore, exploring novel porous matrix with high level of boronic acid integration via a facile, efficient synthesis strategy is of great significance for the practical recognition and separation of CDBs.

Metal–organic frameworks (MOFs), consisting of inorganic nodes and organic ligands, are booming as fascinating porous crystalline materials. In comparison with conventional inorganic porous solids, MOFs feature high surface area, adjustable pore sizes, and versatile framework compositions.[21–23] Moreover, the organic ligand component of MOFs allows fine-tuning of the pore environment with favorable implications on properties.[24–27] In virtue of such characteristics, MOFs have emerged as a new class of outstanding platform for the adsorption of target molecules ranging from gas species to biological molecules.[28–39] Inspired by these studies, it is reasonable to suppose that boronic acid modified MOFs might be potentially promising for selective recognition and subsequently separation of CDBs. Nevertheless, up till now, no report has been found to address this topic. This could be probably ascribed to three reasons: 1) there is a lack of suitable boronic acid containing ligands for the synthesis of functionalized MOFs, and the modification of ligands is often tedious; 2) generally, the additional functional groups occupy

Dr. X. Y. Zhu, Prof. J. L. Gu, Prof. Y. S. Li, Prof. J. L. Shi
Key Laboratory for Ultrafine Materials of Ministry of Education
School of Materials Science and Engineering
East China University of Science and Technology
Shanghai 200237, China
E-mail: jinlougu@ecust.edu.cn
J. Y. Zhu, Dr. L. M. Zhao
State Key Laboratory of Bioreactor Engineering
R&D Center of Separation and Extraction Technology in Fermentation Industry
East China University of Science and Technology
Shanghai 200237, China

DOI: 10.1002/adfm.201500587

more space, leading to significant reductions in molecule-accessible surface area and pore volumes of the resultant MOFs; and 3) very few MOFs feature high chemical stability under base/acid conditions for CDBs binding and subsequent dissociation. Thus, it is highly desirable to develop new MOFs simultaneously integrated with the merits of accessible boronic acid functionality, good chemical stability, and high porosity using readily available boronic acid containing compounds.

We notice that the recently developed metal–ligand–fragment coassembly (MLFC) strategy could effectively work to introduce a wide variety of functional groups into MOFs, in which the primitive ligand and its fragment were cocrystallized into the framework.[40–42] The resulted new MOFs maintain the isostructure of the parent framework derived from only the primitive ligand.[42] Since the fragment ligands have fewer coordination groups than the primitive one, they play a role in breaking a wall between neighboring pores. In this domain, decoration of the frameworks with bulky functionalities could be facilitated. Obviously, depending on the functional groups on the ligand fragments, the MOFs can be functionalized without causing reduction in pore volume.[42] These advantages of the linker fragmentation approach rationalize the possibility of incorporating the boronic acid containing fragment into MOFs, and might offer a new platform for realizing CDBs recognition and sequestration. Because of their giant pores (with free diameters of 25 and 29 Å) for the free mass diffusion of CDBs,[43] Cr-based MOFs of MIL-100 (MIL stands for Materials from Institut Lavoisier) would be an ideal choice to exemplify the elaboration of boronic acid functionalized MOFs (MIL-100-B). Additionally, their well-known excellent chemical stability could bear the ligand fragmentation, which leads to incomplete connectivity between the ligands and metal nodes.[44,45]

In the current work, we report the facile preparation of this new MOFs of MIL-100-B with active boronic acid suspended in their cavities via the MLFC approach in which commercially available 5-boronobenzene-1,3-dicarboxylic acid (BBDC) was employed as ligand fragment to introduce functional component. The amount of boronic acid group on MIL-100-B could be systematically tuned by changing the feed ratios of BBDC to primitive ligand of 1,3,5-benzene tricarboxylic acid (BTC) in the reactant mixtures. The obtained MOFs exhibit comparable surface areas and pore volumes with parent MIL-100 even at BBDC/BTC feed ratio of 1:1.5, and present exceptional chemical stability in a wide pH range. As expected, the inherent boronic components in cavities could effectively serve as the recognition units for the *cis*-diol moieties and consequently enhance the capture capabilities of the elaborated MIL-100-B for CDBs. The binding and dissociation between MIL-100-B and CDBs could be reversibly switched by changing the pH conditions. Even after three consecutive mild basic and acid treatments for the binding and dissociation of representative CDBs, the crystalline structure of the resultant MOFs is still well preserved. The exceptional chemical stability, high porosity, and good reusability as well as the intrinsic *cis*-diol moieties recognition function prefigure the great potentials of the current MIL-100-B in CDBs purification, sensing, and separation applications.

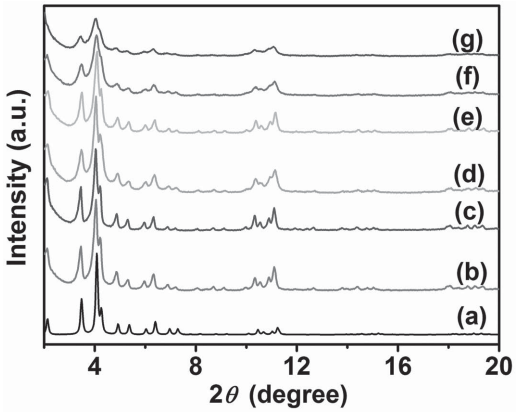

Figure 1. Powder XRD patterns for a) the simulated MIL-100, b) the as-synthesized MIL-100 and MIL-100-B synthesized in different feed ratios of BBDC to BTC from c) 1:9, d) 1:4, e) 1:2.3, f) 1:1.5 to g) 1:1.

2. Results and Discussion

2.1. Characterization of MIL-100-B

The MIL-100-B was prepared through the direct hydrothermal reaction between chromium and a mixture of BTC (primitive ligand) and BBDC (ligand fragment). To maximize the incorporation of fragments without changing the structure of the parent frameworks, various feed ratios of BBDC to BTC were applied. We employed the XRD technique to characterize the structural evolvement of the synthesized MOFs with feed ratios of BBDC to BTC from 1:9 to 1:1 (**Figure 1**). All the samples exhibit the similar Bragg diffraction peaks in consistence with the simulated pattern (Figure 1a), demonstrating that the crystalline materials are formed with isostructure to the parent framework.[41,42] However, for the feed ratio 1:1.5 of BBDC to BTC, the crystalline MIL-100-B presents slightly broadened and weakened XRD peaks, which might be due to the slightly decreased framework crystallinity. Further increasing the feed ratio of BBDC to BDC up to 1:1 still yields crystalline MOFs but with more diminished XRD peak intensity (Figure 1g).

XPS spectra of three MIL-100-B samples (BBDC/BTC feed ratios of 1:4, 1:2.3, and 1:1.5) were collected to verify the integration of boronic acid units. All the peaks at 192.0 eV in wide scan XPS spectra (**Figure 2**a–c) undoubtedly disclose the presence of B element derived from BBDC. In addition, the intensities of B signal increase with the increase of BBDC/BTC feed ratio. The C1s XPS spectra could provide further information about the introduced functional groups on MIL-100-B. For a BBDC/BTC ratio of 1:4, the deconvoluted C1s peak (Figure 2d) consists of four peaks, which could be assigned to C in C-B (283.9 eV), C-C/C=C (284.6 eV), C-O (285.7 eV), and O-C=O (288.5 eV), respectively.[46–48] Similar peaks could be observed in the deconvoluted C1s peak of MOFs with BBDC/BTC feed ratios of 1:2.3 (Figure 2e) and 1:1.5 (Figure 2f). With the increase in BBDC/BTC feed ratios, the intensities for the peaks corresponding to the C-O (285.7 eV) and O-C=O (288.5 eV) diminish. Meanwhile, the intensity for C-B (283.9 eV) signal enhances corresponding to the higher relative content of BBDC in MOFs in good agreement with the deduction from boron signals in wide scan XPS

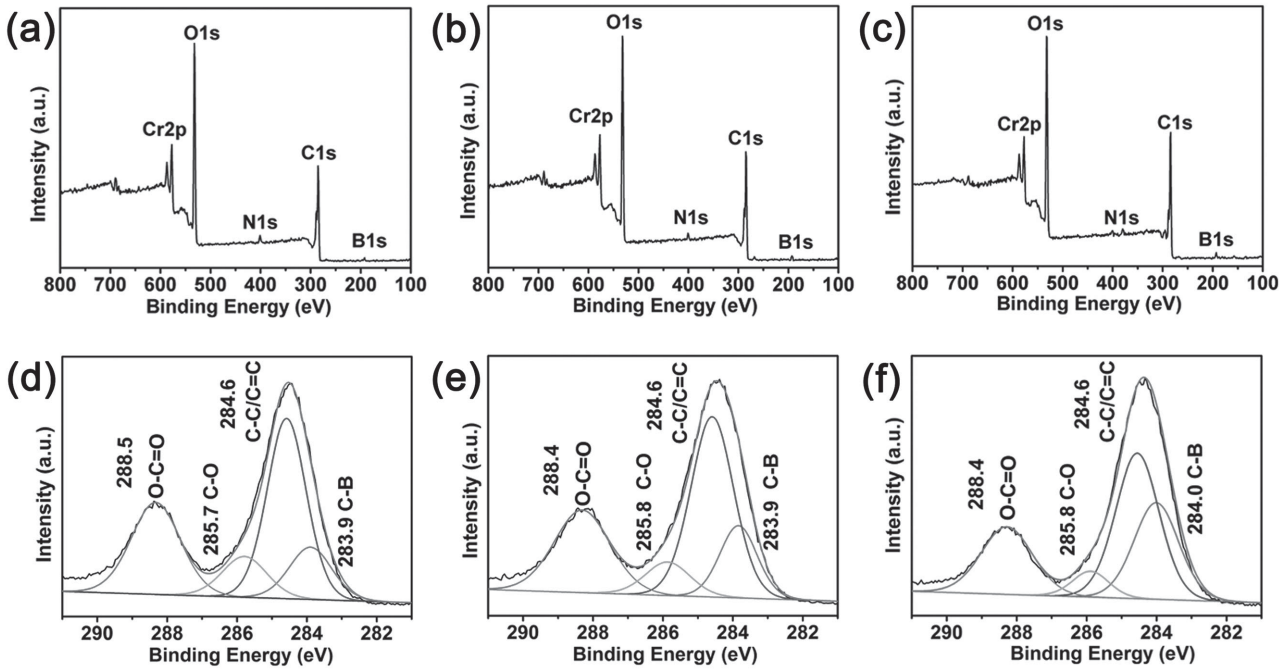

Figure 2. Wide scan XPS spectra of MIL-100-B synthesized in BBDC/BTC feed ratios of a) 1:4, b) 1:2.3, and c) 1:1.5. The magnified C1s XPS spectra of MIL-100-B synthesized in feed ratios of BBDC to BTC at d) 1:4, e) 1:2.3, and f) 1:1.5.

profiles. These results clearly manifest that BBDC has been successfully incorporated into the MOFs, and the amount of the incorporated functional group could be facilely tuned by changing the BBDC content in the initial reactant mixture.

To precisely determine the quantity of BBDC in MIL-100-B crystals, ^{11}B NMR spectra were recorded. 15 mg of sample was digested in $NaOD/D_2O$ and the digest was treated with centrifugation. 2 mg of $NaBF_4$ was added to the supernatant as an internal standard.[49] Then, the mixture was transferred into a synthetic quartz NMR tube ($B < 0.01$ ppm) for ^{11}B NMR analysis. As shown in **Figure 3**A, two ^{11}B NMR signals could be clearly identified at –17.3 and –20.4 ppm, assigning to B elements in BBDC and $NaBF_4$, respectively. Through comparing integrations of the BBDC and $NaBF_4$ resonances,[49] it is found that approximate 80% BBDC is included into the framework at a BBDC/BTC feed ratio of 1:9, which is quantified to be 0.24 mmol boronic acid group per gram MIL-100-B crystal (Figure 3B). For BBDC/BTC feed ratios of 1:4, 1:2.3, 1:1.5, and 1:1, the quantities of BBDC in the MOF crystals are calculated to be 0.45, 0.55, 0.62, and 0.65 mmol g^{-1}. It should be pointed out that the BBDC amounts in MIL-100-B are not linearly correlated with the ones in feed, and its incorporation is close to saturation at a BBDC/BTC feed ratio of 1:1 (Figure 3Ba).

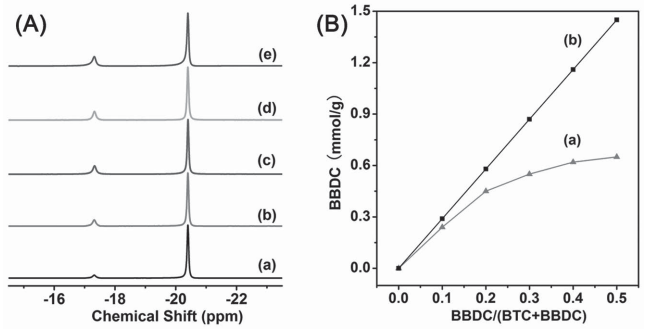

Figure 3. A) The ^{11}B NMR spectra of digestion products of MIL-100-B synthesized in different feed ratios of BBDC to BTC at a) 1:9, b) 1:4, c) 1:2.3, d) 1:1.5, and e) 1:1 in alkaline D_2O solution. $NaBF_4$ was used as an internal standard (–20.4 ppm). B) The effect of BBDC content in the initial reactant mixture on the amount of boronic acid group in the MIL-100-B crystals: a) experimental and b) theoretical data corresponding to the BBDC in crystals and feed, respectively.

TEM was used to investigate the morphology evolvement of the synthesized MIL-100-B with different BBDC/BTC feed ratios. It can be observed that the parent MIL-100 is in irregular shape, and the particle size is in submicrometer scale (**Figure 4**a). On the contrast, the discrete particles with relatively uniform size and shape are obtained in the presence of low level of BBDC/BTC feed ratio (Figure 4b). This regular nanoscale particle could facilitate the accessibility of the boronic acid groups in the resultant MIL-100-B benefiting from the short diffusion pathway for the guest molecules. Upon increasing the BBDC/BTC feed ratio from 1:9 to 1:2.3, the average particle size is reduced from ≈270 to 160 nm (Figure 4b–d). However, further incorporating BBDC yields a negative impact on morphology evolvement, and leads to ill-defined particle shape (Figure 4e,f).

N_2 sorption analysis was adopted to evaluate the textural parameters of the obtained MIL-100-B. The N_2 adsorption–desorption curves for all the samples exhibit the characteristic steps and type IV isotherm in agreement with the observation for MIL-100 structures (**Figure 5**).[50] This further affirms the fact that the inclusion of BBDC did not destroy the structure of parent framework. BET surface areas of the materials resulting

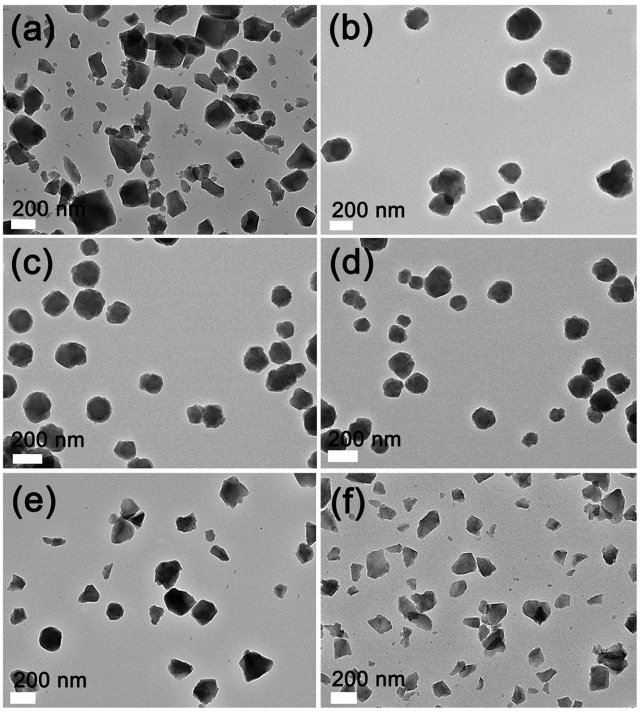

Figure 4. TEM images of a) parent MIL-100 and MIL-100-B synthesized with BBDC/BTC feed ratios of b) 1: 9, c) 1:4, d) 1:2.3, e) 1:1.5, and f) 1:1.

from BBDC/BTC feed ratios of 1:4 and 1:2.3 are calculated to be 1628 and 1603 m^2 g^{-1}, which are comparable to the value of unfunctionalized MOFs (1646 m^2 g^{-1}). Pore volumes for these samples also present the similar variation trend (**Table 1**). These large surface areas and pore volumes should attribute to the inherent characteristics of the MLFC synthesis approach since the boronic acid groups are pointing toward the pores generated via the linker fragmentation. On contrast, in most traditional functionalization methods for MOFs, functionalized groups generally dangle into the pore space and result in decreased pore size and surface areas. For a BBDC/BTC feed ratio of 1:1.5, the MIL-100(Cr)-B still feature considerable surface area (1452 m^2 g^{-1}) though a slight reduction in porosity is observed. Meanwhile, the porosity further diminishes

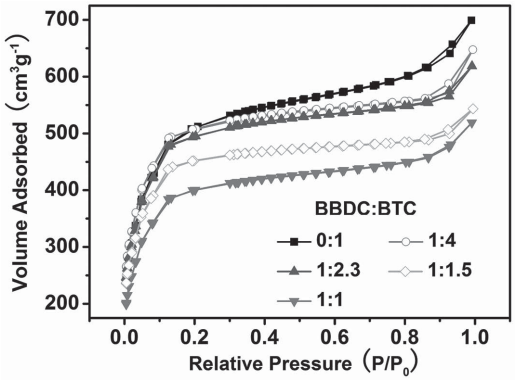

Figure 5. N_2 adsorption–desorption isotherms of MIL-100-B synthesized in different BBDC/BTC feed ratios.

Table 1. Textural parameters of parent MIL-100 and MIL-100-B synthesized in BBTC/BTC feed ratios of 1:4, 1:2.3, 1:1.5, and 1:1.

BBDC:BTC	S_{BET} [m^2 g^{-1}]	V_P [cm^3 g^{-1}]
0:1	1646	1.05
1:4	1628	0.92
1:2.3	1603	0.90
1:1.5	1452	0.83
1:1	1277	0.72

with increasing BBDC/BTC feed ratio to 1:1, which might be resulted from the weakened framework crystallinity as confirmed by the XRD pattern. Taking above-mentioned results together, we determined that the BBDC/BTC feed ratios of 1:4, 1:2.3, and 1:1.5 are optimal for the fabrication of MIL-100-B to achieve the good crystallinity of framework, considerable boronic acid inclusion level, well-defined particle morphology, and high surface area.

On the basis of the excellent chemical stability of parent Cr-based MIL-100,[43,51] we expect that the currently developed MIL-100-B could be chemically resistant under acidic and mild basic conditions. To test their chemical stability, MIL-100-B samples synthesized with BBDC/BTC feed ratios of 1:2.3 and 1:1.5 were soaked in aqueous solutions with different pH values for 24 h.[52] After that, those MOFs were collected by centrifugation and dried at 100 °C in vacuum. XRD patterns (**Figure 6** and Figure S1, Supporting Information) elucidate that MIL-100-B remains intact upon these treatments in accordance with our expectation. This exceptional chemical stability, combining with the merits of high porosity, accessible boronic acid groups, would make the newly elaborated MOFs applicable for the recognition and subsequent sequestration of CBDs.

2.2. The Effects of Boronic Acid Content and pH on the Interaction between MIL-100-B and CDBs

As a proof of principle, we first investigated the effect of the boronic acid content on their extraction capabilities for CDBs from aqueous solution with the elaborated MIL-100-B.

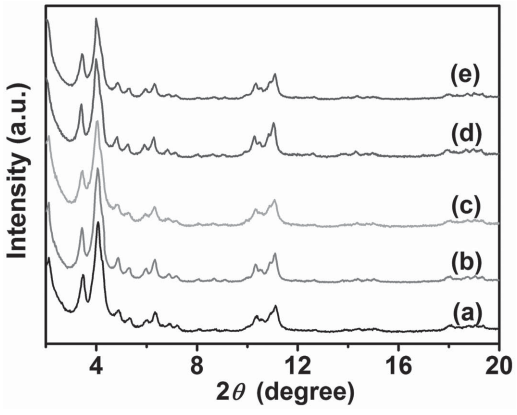

Figure 6. XRD patterns for a) MIL-100-B synthesized with BBDC to BTC feed ratio of 1:1.5 and the samples soaked in aqueous solutions with pH values of b) 0, c) 7, d) 10, and e) 11 for 24 h.

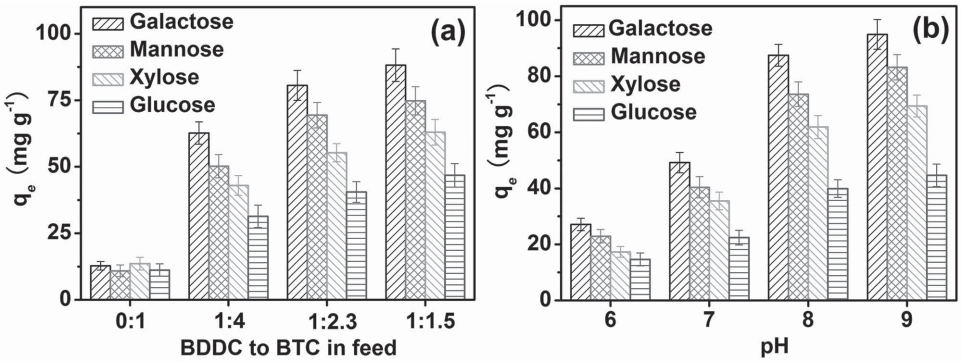

Figure 7. The effects of a) BBDC content and b) pH on the adsorption capacities for the representative CDBs of galactose, mannose, xylose, and glucose over MIL-100 or MIL-100-B (25 °C, $C_{adsorbate}$ = 2 g L^{-1}).

Galactose, mannose, xylose, and glucose, commonly present in biomass,[53] were selected as representative CDBs. After the adsorption for a sufficient time of 24 h at pH 8, the amounts of the adsorbed CDBs on the as-synthesized MOFs were measured by HPLC (**Figure 7**a). It is noticed that the adsorption capacities of the utilized MIL-100-B for the selected CDBs are much higher than that of unfunctionalized MIL-100 and increase with the increase of the incorporated BBDC amounts. These indicate that the integrated boronic acid groups do play vital roles in the adsorption enhancement of CDBs. Therefore, we take MIL-100-B with BBDC/BTC feed ratio of 1:1.5, denoted as MIL-100-B (0.4), as an example to further exploit the adsorption performance. For the examined MIL-100-B samples, we find that galactose could be most effectively adsorbed among all the CDBs applied in the current work. Given the fact that the strength of boronic acid–CDBs interactions is dependent on the structure of CDBs,[49,54] the most distinguished adsorption of galactose in MIL-100-B crystals might be attributed to its relatively high furanose-type isomer content, which facilitates their complexation with boronic acids.[49]

It has been well documented that the interactions between boronic acid and CDBs are also pH dependent.[54] Hence, a slight change in media pH can result in a noticeable change in the affinity between the integrated boronic acid in MIL-100-B and *cis*-diol moieties. To estimate the effects of pH on the adsorption capabilities of galactose, mannose, xylose, and glucose on MIL-100-B (0.4), batches of adsorption experiments were conducted in the pH range from 6 to 9 (Figure 7b). When initial pH is preset at 6, small amounts of CDBs could be absorbed from solutions. The adsorbed amounts of CDBs increase with increasing solution pH and the adsorption capacity of ≈95 mg g^{-1} for galactose could be achieved when the initial solution pH is tuned to 9. This is in good agreement with the general correlation of the boronate affinity with pH,[16,54] further verifying that boronic acid units of MIL-100-B play the significant role in CDBs recognition and capture. Providing that one boronic acid group binds one *cis*-diol moiety, it can be quantified that about 85% of the introduced boronic groups have been worked for the capture of CDBs according to this adsorption capacity at pH 9. The observed pH-dependent CDBs adsorption in the obtained MIL-100-B also suggests that these newly developed adsorbents could be regenerated under acid conditions.

2.3. Physicochemical Parameters Determination after CDBs Occlusion

To get the further knowledge about the structural, textural, and compositional evolvements of the elaborated MOFs upon its interaction with CDBs, we take galactose adsorbed MIL-100-B (0.4) (denoted as MIL-100-B (0.4) Ga) as an example for the discussion in depth. As confirmed by XRD patterns (Figure S2a,b, Supporting Information), the CDBs adsorption did not change the original crystalline structure of MIL-100-B (0.4), indicating that the resultant MOFs are chemically tolerant to the adsorption environment. The nitrogen adsorption–desorption curve for MIL-100-B (0.4) Ga displays typical IV isotherm (Figure S3, Supporting Information), further verifying the fact that the CDBs treatment did not destroy the structure integrity of the applied MOFs. Furthermore, the decreases in the surface area and pore volume are observed after galactose adsorption, due to the trapping of the adsorbate molecules in the cages of MOFs. FT-IR spectra (Figure S4, Supporting Information) affirm the occlusion of galactose in the MIL-100-B (0.4) after the adsorption experiment as judged from the appearance of new bands at around 2950 cm^{-1} in the spectrum of MIL-100-B (0.4) Ga, which could be assigned to the C-H bonds in the galactose molecules.

TGA was used to estimate the galactose content in MIL-100-B (0.4) Ga (**Figure 8**). The adsorbed galactose should burn out along with the decomposition of organic ligands from

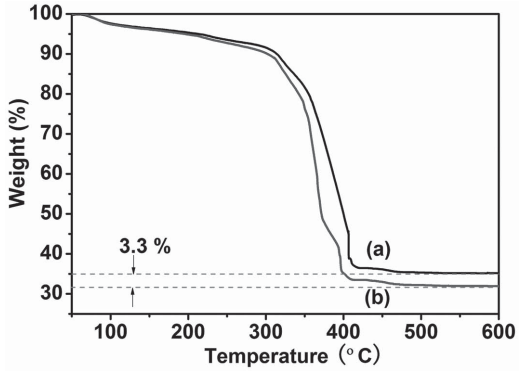

Figure 8. TGA profiles of a) MIL-100-B (0.4) and b) galactose adsorbed MIL-100-B (0.4).

the framework, which occurs between 275 and 450 °C.[45,50] The residues are identified to be Cr_2O_3 and B_2O_3 when temperature reaches 550 °C. The preserved weight percentage at 550 °C for MIL-100-B (0.4) is 35.3% while that for galactose adsorbed sample is 32%. Based on these values at 550 °C, the galactose content in 1 g of the newly developed MOFs could be determined to be ≈93 mg, well consistent with the adsorption amount measured by HPLC.

To shed light on the molecular interaction of CDBs with newly elaborated boronic- acid-functionalized MOFs, the MIL-100-B (0.4) Ga was digested in $NaOD/D_2O$, and analyzed by ^{11}B NMR spectroscopy (Figure S5, Supporting Information). For pristine MIL-100-B (0.4), a single signal at –17.3 ppm in the range of –10 to –18 ppm could be assigned to B element in free BBDC. After galactose adsorption, a broad resonance signal centered at –12.4 ppm and a small peak at –17.9 ppm appear in the spectrum, which might be characteristic of the five- and six-membered B-diol esters, respectively.[55] This indicates that the CDBs are sequestrated by the currently developed MOFs through the affinity reaction between *cis*-diol moieties and the accessible boronic acid units in accordance with our proposal.

2.4. Recycle Investigation

For the practical applications such as sensing and separation, regeneration characteristics of the currently developed MOFs are of great importance. To evaluate the desorption of CDBs from MIL-100-B, MIL-100-B (0.4) Ga was soaked in 0.1 M HNO_3 aqueous solution and shaken at 25 °C for 5 h. After acid treatment, more than 95% of the adsorbed galactose could be stripped from the boronic acid containing MOFs, suggesting that MIL-100-B (0.4) can be effectively regenerated under relatively mild acidic conditions. The recycle of MIL-100-B for CDBs capture was then investigated. It is observed that the adsorption capacity of current MOFs for galactose slightly decreases from 94.2 to 81.7 mg g^{-1} with increasing times of the reuse (Figure S6, Supporting Information). Moreover, even after three consecutive adsorption runs, the crystalline structure is still preserved as verified by XRD technique (Figure S2c, Supporting Information). These results elucidate the excellent reusability of MIL-100-B (0.4) as a promising candidate for CDBs recognition and subsequent separation.

3. Conclusions

In summary, new MOFs with accessible boronic acid group suspended in cavities have been successfully synthesized via MLFC strategy, in which commercially available ligand fragment of BBDC is used to introduce functional components. The integrated boronic acid content could be systematically modulated and the crystalline structure of the obtained MOFs remains intact in a wide pH range. Thanks to their inherent boronic acid group, exceptional chemical stability, as well as high porosity, MIL-100-B offers a new platform for the effective recognition and subsequent separation of CDBs from aqueous solution with not only high adsorption capacities but also good reusability. Except the current investigated typical CDBs of galactose, mannose, xylose, and glucose, the newly explored MIL-100-B could be hopefully expanded for the isolation of a wide range of CDBs. Furthermore, given the wide potential use of boronic acid group in separation, targeted drug delivery,[56] sensing,[57] and synthetic organic chemistry,[58] our proposed synthesis strategy could be facilely adopted to incorporate boronic acid units into a wide range of MOFs for these applications.

4. Experimental Section

Materials: 1,3,5-Benzene tricarboxylic acid (BTC), metallic chromium, and representative CDBs including galactose, mannose, xylose, and glucose were purchased from Aladdin Chemistry Co., Ltd. (Shanghai, China). *N*,*N*-dimethylformamide (DMF), HF (40%), and ethanol were received from Shanghai Chemical Reagents Company. 5-Boronobenzene-1,3-dicarboxylic acid (BBDC) was purchased from Energy Chemical Reagents Company. Synthetic quartz NMR tubes ($B < 0.01$ ppm) were purchased from American Norell Company.

Characterizations: Powder X-ray diffraction (XRD) patterns were acquired at a rate of 6° min^{-1} over the range of 2–20° (2θ) on Bruker D8 equipped with Cu Kα radiation (40 kV, 40 mA). X-ray photoelectron spectroscopy (XPS) signals were collected on a VG Micro-MK II instrument. N_2 adsorption–desorption isotherms were collected with a Quantachrome NOVA 4200E porosimeter at –196 °C. All the samples were degassed under vacuum for 12 h before measurements. The specific surface area and micropore volume were calculated by the Brunauer–Emmett–Teller (BET) method. Transmission electron microscopy (TEM) images were taken on a JEOL JEM-2100 microscope operating at 200 kV. ^{11}B NMR spectra were recorded on a Bruker spectrometer operating at 500 MHz. FT-IR spectra were carried out on Nicolet 7000-C spectroscopy using the KBr method. Thermogravimetric analysis (TGA) was conducted on a Perkin-Elmer thermogravimetric analyzer by heating the sample to 800 °C under air atmosphere (50 mL min^{-1}) at a heating rate of 10 °C min^{-1}. The samples were degassed in vacuo at 120 °C for 12 h before TGA analysis.

Synthesis of MIL-100-B: To synthesize MIL-100-B with different contents of boronic acid groups, the starting materials of metallic chromium (52 mg, 1 mmol), BBDC (0.67x mmol; x = 0, 0.1, 0.2, 0.3, 0.4, and 0.5), BTC (0.67(1 – x) mmol), and H_2O (4.8 mL, 0.267 mol) were introduced into a 25 mL Teflon reactor. After stirring for 2 h, HF (0.5 mmol) was added to the mixture. The resulted solution was stirred for another 0.5 h, and then the reactor was sealed and heated in an oven at 200 °C for 72 h. After cooled down to room temperature, the obtained green solid was collected by centrifugation and soaked in DMF at room temperature for 2 h to remove the free BTC and BBDC. The same procedure was repeated three times using alkaline aqueous solution instead of DMF to remove the fluoride.[59] Then, the obtained green solid was washed with acetone before drying at 100 °C under vacuum for 24 h.

CDBs Adsorption Experiments: The function of boronic acid groups was testified by a batch of adsorption experiments that were conducted at room temperature (25 °C) by utilizing representative CDBs such as galactose, xylose, mannose, and glucose as the adsorbates. Aqueous stock solutions (20 g L^{-1}) of galactose, mannose, xylose, and glucose were prepared by dissolving the CDBs in deionized water and the test solutions were made by the subsequent dilution of the stock solutions. Before adsorption, the MIL-100-B were dried at 120 °C in vacuum for 12 h and kept in a desiccator. The pH values were adjusted with negligible amount of 0.1 M HNO_3 or 0.1 M NaOH. The experiments were conducted at pH range of 6–9 with an initial adsorbate concentration of 2.0 g L^{-1} and the adsorbent concentration was fixed at 1.5 g L^{-1}. The mixtures of saccharide solutions and MIL-100-B suspensions were placed in a platform shaker at a shaking speed of 180 rpm. The residual CDBs in a series of independent solutions were measured after a sufficient adsorption time of 24 h. Then, the samples were centrifuged

and the supernatants were filtered using membrane filters with a pore size of 0.22 μm. The concentrations of galactose, mannose, xylose, or glucose were determined by high performance liquid chromatography (HPLC, Agilent 1120) using a Water Sugar-Pak1 column and an Agilent 1260 Infinity refractive index detector (RID).

Regeneration Experiments: After the adsorption experiments, the used MIL-100-B was separated by centrifugation, and dried at 100 °C. Then, the CDBs-occluded MOFs were added into 6 mL of 0.1 M HNO_3 aqueous solution and shaken at 25 °C for 5 h. Finally, the desorbed MIL-100-B was washed with pure water twice, and dried for reusing. To investigate the reusability of the currently developed MOFs for the adsorption of CDBs, 9 mg of regenerated MIL-100-B was dispersed in 6 mL of 2 g L^{-1} galactose. After adsorption at pH 9 for 12 h, the mixture was centrifuged and the supernatants were filtered using membrane filters with a pore size of 0.22 μm. The concentration of galactose in the filtrate was measured by HLPC.

Supporting Information

Supporting Information is available from the Wiley Online Library or from the author.

Acknowledgements

This work was financially supported by the Natural Science Foundation of China (51072053, 51372084, 51132009), the Innovation Program of Shanghai Municipal Education Commission (13zz040), the Nano-Special Foundation for Shanghai Committee of Science and Technology (12nm0502600), and the 111 Project (B14018).

Received: February 11, 2015
Revised: April 17, 2015
Published online: May 15, 2015

[1] C. R. Bertozzi, L. L. Kiessling, *Science* **2001**, *291*, 2357.
[2] A. Varki, *Glycobiology* **1993**, *3*, 97.
[3] L. Lehle, S. Strahl, W. Tanner, *Angew. Chem. Int. Ed.* **2006**, *45*, 6802.
[4] R. G. Spiro, *Glycobiology* **2002**, *12*, 43R.
[5] N. Schweigert, A. J. B. Zehnder, R. I. L. Eggen, *Environ. Microbiol.* **2001**, *3*, 81.
[6] Y. Jiang, Y. Ma, *Anal. Chem.* **2009**, *81*, 6474.
[7] Y. Liu, L. Ren, Z. Liu, *Chem. Commun.* **2011**, *47*, 5067.
[8] R. Nishiyabu, Y. Kubo, T. D. James, J. S. Fossey, *Chem. Commun.* **2011**, *47*, 1106.
[9] G. Springsteen, B. Wang, *Chem. Commun.* **2001**, 1608.
[10] P. R. Westmark, S. J. Gardiner, B. D. Smith, *J. Am. Chem. Soc.* **1996**, *118*, 11093.
[11] G. Springsteen, B. Wang, *Tetrahedron* **2002**, *58*, 5291.
[12] H. G. Kuivila, A. H. Keough, E. J. Soboczenski, *J. Org. Chem.* **1954**, *19*, 780.
[13] S. T. Wang, D. Chen, J. Ding, B. F. Yuan, Y. Q. Feng, *Chem. Eur. J.* **2013**, *19*, 606.
[14] K. Yum, J.-H. Ahn, T. P. McNicholas, P. W. Barone, B. Mu, J.-H. Kim, R. M. Jain, M. S. Strano, *ACS Nano* **2012**, *6*, 819.
[15] L. Zhang, Y. Xu, H. Yao, L. Xie, J. Yao, H. Lu, P. Yang, *Chem. Eur. J.* **2009**, *15*, 10158.
[16] S. Mohapatra, N. Panda, P. Pramanik, *Mater. Sci. Eng. C* **2009**, *29*, 2254.
[17] L. Liu, Y. Zhang, L. Zhang, G. Yan, J. Yao, P. Yang, H. Lu, *Anal. Chim. Acta* **2012**, *753*, 64.
[18] Y.-H. Zhao, D. F. Shantz, *Langmuir* **2011**, *27*, 14554.
[19] Y. Xu, Z. Wu, L. Zhang, H. Lu, P. Yang, P. A. Webley, D. Zhao, *Anal. Chem.* **2009**, *81*, 503.
[20] S. Senel, S. T. Camli, M. Tuncel, A. Tuncel, *J. Chromatogr. B* **2002**, *769*, 283.
[21] O. M. Yaghi, M. O'Keeffe, N. W. Ockwig, H. K. Chae, M. Eddaoudi, J. Kim, *Nature* **2003**, *423*, 705.
[22] S. Kitagawa, R. Kitaura, S. I. Noro, *Angew. Chem. Int. Ed.* **2004**, *43*, 2334.
[23] G. Férey, *Chem. Soc. Rev.* **2008**, *37*, 191.
[24] M. Lammert, S. Bernt, F. Vermoortele, D. E. De Vos, N. Stock, *Inorg. Chem.* **2013**, *52*, 8521.
[25] H. Deng, C. J. Doonan, H. Furukawa, R. B. Ferreira, J. Towne, C. B. Knobler, B. Wang, O. M. Yaghi, *Science* **2010**, *327*, 846.
[26] M. Kandiah, M. H. Nilsen, S. Usseglio, S. Jakobsen, U. Olsbye, M. Tilset, C. Larabi, E. A. Quadrelli, F. Bonino, K. P. Lillerud, *Chem. Mater.* **2010**, *22*, 6632.
[27] M. Eddaoudi, J. Kim, N. Rosi, D. Vodak, J. Wachter, M. O'Keeffe, O. M. Yaghi, *Science* **2002**, *295*, 469.
[28] T. Rodenas, M. van Dalen, E. García-Pérez, P. Serra-Crespo, B. Zornoza, F. Kapteijn, J. Gascon, *Adv. Funct. Mater.* **2014**, *24*, 249.
[29] D. Liu, H. Wu, S. Wang, Z. Xie, J. Li, W. Lin, *Chem. Sci.* **2012**, *3*, 3032.
[30] B. Panella, M. Hirscher, H. Pütter, U. Müller, *Adv. Funct. Mater.* **2006**, *16*, 520.
[31] X. Y. Zhu, B. Li, J. Yang, Y. Li, W. Zhao, J. Shi, J. L. Gu, *ACS Appl. Mater. Interfaces* **2015**, *7*, 223.
[32] J.-Q. Jiang, C.-X. Yang, X.-P. Yan, *ACS Appl. Mater. Interfaces* **2013**, *5*, 9837.
[33] K. A. Cychosz, A. G. Wong-Foy, A. J. Matzger, *J. Am. Chem. Soc.* **2008**, *130*, 6938.
[34] E. Haque, J. W. Jun, S. H. Jhung, *J. Hazard. Mater.* **2011**, *185*, 507.
[35] X. Y. Zhu, J. L. Gu, Y. Wang, B. Li, Y. Li, W. Zhao, J. Shi, *Chem. Commun.* **2014**, *50*, 8779.
[36] D. Cunha, M. Ben Yahia, S. Hall, S. R. Miller, H. Chevreau, E. Elkaïm, G. Maurin, P. Horcajada, C. Serre, *Chem. Mater.* **2013**, *25*, 2767.
[37] P. A. P. Mendes, P. Horcajada, S. Rives, H. Ren, A. E. Rodrigues, T. Devic, E. Magnier, P. Trens, H. Jobic, J. Ollivier, G. Maurin, C. Serre, J. A. C. Silva, *Adv. Funct. Mater.* **2014**, *24*, 7666.
[38] R. El Osta, A. Carlin-Sinclair, N. Guillou, R. I. Walton, F. Vermoortele, M. L. Maes, D. de Vos, F. Millange, *Chem. Mater.* **2012**, *24*, 2781.
[39] A. Saeed, F. Maya, D. J. Xiao, M. Najam-ul-Haq, F. Svec, D. K. Britt, *Adv. Funct. Mater.* **2014**, *24*, 5790.
[40] Z. Fang, J. P. Dürholt, M. Kauer, W. Zhang, C. Lochenie, B. Jee, B. Albada, N. Metzler-Nolte, A. Pöppl, B. Weber, M. Muhler, Y. Wang, R. Schmid, R. A. Fischer, *J. Am. Chem. Soc.* **2014**, *136*, 9627.
[41] G. Barin, V. Krungleviciute, O. Gutov, J. T. Hupp, T. Yildirim, O. K. Farha, *Inorg. Chem.* **2014**, *53*, 6914.
[42] J. Park, Z. U. Wang, L.-B. Sun, Y.-P. Chen, H.-C. Zhou, *J. Am. Chem. Soc.* **2012**, *134*, 20110.
[43] M. Tong, D. Liu, Q. Yang, S. Devautour-Vinot, G. Maurin, C. Zhong, *J. Mater. Chem. A* **2013**, *1*, 8534.
[44] K. A. Cychosz, A. J. Matzger, *Langmuir* **2010**, *26*, 17198.
[45] G. Férey, C. Serre, C. Mellot-Draznieks, F. Millange, S. Surblé, J. Dutour, I. Margiolaki, *Angew. Chem.* **2004**, *116*, 6456.
[46] L. Song, J. Zhao, S. Luan, J. Ma, J. Liu, X. Xu, J. Yin, *ACS Appl. Mater. Interfaces* **2013**, *5*, 13207.
[47] G. Zhao, L. Jiang, Y. He, J. Li, H. Dong, X. Wang, W. Hu, *Adv. Mater.* **2011**, *23*, 3959.
[48] S. Y. Kim, J. Park, H. C. Choi, J. P. Ahn, J. Q. Hou, H. S. Kang, *J. Am. Chem. Soc.* **2007**, *129*, 1705.

[49] M. Shimomura, B. Ono, K. Oshima, S. Miyauchi, *Polymer* **2006**, *47*, 5785.
[50] P. Horcajada, C. Serre, M. Vallet-Regí, M. Sebban, F. Taulelle, G. Férey, *Angew. Chem.* **2006**, *118*, 6120.
[51] Z.-Y. Gu, Y.-J. Chen, J.-Q. Jiang, X.-P. Yan, *Chem. Commun.* **2011**, *47*, 4787.
[52] H.-L. Jiang, D. Feng, K. Wang, Z.-Y. Gu, Z. Wei, Y.-P. Chen, H.-C. Zhou, *J. Am. Chem. Soc.* **2013**, *135*, 13934.
[53] P. Saari, H. Heikkilä, M. Hurme, *J. Chem. Eng. Data* **2010**, *55*, 3462.
[54] C. Lü, H. Li, H. Wang, Z. Liu, *Anal. Chem.* **2013**, *85*, 2361.
[55] K. Djanashvili, L. Frullano, J. A. Peters, *Chem. Eur. J.* **2005**, *11*, 4010.
[56] Y. Zhao, B. G. Trewyn, I. I. Slowing, V. S.-Y. Lin, *J. Am. Chem. Soc.* **2009**, *131*, 8398.
[57] B. Fabre, L. Taillebois, *Chem. Commun.* **2003**, 2982.
[58] A. Suzuki, *Angew. Chem. Int. Ed.* **2011**, *50*, 6722.
[59] Q. Liu, K. Xiao, L. Wen, Y. Dong, G. Xie, Z. Zhang, Z. Bo, L. Jiang, *ACS Nano* **2014**, *8*, 12292.